Aryl-substituted acridine donor derivatives modulate the transition dipole moment orientation and exciton harvesting properties of donor-acceptor thermally activated delayed fluorescence emitters, leading to highly efficient OLEDs.

Ettore Crovini,[a] Kleitos Stravou,*[b] Prakhar Sahay,[c] Binh Minh Nguyễn,[c] Thomas Comerford,[a] Stuart Warriner,[d] Wolfgang Brütting,*[c] Andrew Monkman,*[b] and Eli Zysman-Colman*[a]

[a] Organic Semiconductor Centre, EaStCHEM School of Chemistry, University of St Andrews, St Andrews, Fife, KY16 9ST, UK. E-mail: eli.zysman-colman@st-andrews.ac.uk; Web: http://www.zysman-colman.com; Tel: +44 (0)1334 463826.
[b] OEM group, Department of Physics, Durham University, South Road, Durham DH1 3LE, United Kingdom.
[c] Experimental Physics IV, Institute of Physics, University of Augsburg, Augsburg, Germany.
[d] School of Chemistry, University of Leeds, Woodhouse Lane, Leeds LS2 9JT, United Kingdom.

Abstract

Thermally activated delayed fluorescence (TADF) compounds are highly attractive as sensitising and emitting materials for organic light-emitting diodes (OLEDs) as they can harvest both singlet and triplet excitons and convert them into light. In this study we designed a series of derivatives of the widely studied donor-acceptor TADF emitter **DMAC-TRZ** with the objective of correlating their structure to their propensity to orient horizontally in vacuum-deposited doped thin films. This is important as the preferential horizontal orientation of the transition dipole moment (TDM) of the emitter, which tends to co-align with the long axis of D-A compounds, leads to enhanced light-outcoupling, and therefore higher maximum external quantum efficiencies (EQE_{max}) of the OLED. The decoration of the DMAC donor with substituted aryl groups also affects the emission color and the capacity for the emitters to efficiently harvest triplet excitons. The presence of electron-withdrawing 4-cyanophenyl and 4-trifluoromethylphenyl groups in, respectively, **CNPh-DMAC-TRZ** and **CF3Ph-DMAC-TRZ** blue-shifts the emission spectrum but slows down the reverse intersystem crossing rate constant (k_{RISC}), while the opposite occurs in the presence of electron-donating groups in **tBuPh-DMAC-TRZ** and **OMePh-DMAC-TRZ** (red-shifted emission spectrum and faster k_{RISC}). In contrast to our expectations, the OLED performance of the five DMAC-TRZ derivatives does not scale with their degree of horizontal emitter orientation but follows the k_{RISC}

rates. This, in turn, demonstrates that triplet harvesting (and not horizontal emitter orientation) is the dominant effect for device efficiency. Nonetheless, highly efficient OLEDs were fabricated with **tBuPh-DMAC-TRZ** and **OMePh-DMAC-TRZ** as emitters, with improved EQE_{max} (~ 28%) compared to the reference **DMAC-TRZ** devices.

Introduction

Organic light-emitting diodes (OLEDs) are steadily becoming the dominant display technology across a range of consumer electronic markets such as smart watches, mobile phones, and televisions. This is thanks to their excellent power efficiency, that they are light in weight, they can produce both saturated colors necessary for ultra-high definition displays as well as true black, and they can be fabricated on a panoply of substrates, including those that are flexible and transparent.[1,2] OLEDs are based on a multi-layer structure of organic semiconductors sandwiched between two electrodes, where the light-emission results from the electroluminescence of the emitter. The application of current to the device injects electrons and generates holes, which migrate through the device via a so-called hopping mechanism. When these recombine then an exciton is formed, and it is the radiative decay of the exciton that is responsible for the light that ultimately emanates from the OLED. Based on the statistics of spin multiplicity, 25% of the exciton formed by their recombination will have singlet multiplicity, and 75% will have triplet multiplicity. In fluorescent compounds the singlet exciton can decay radiatively, while the triplet exciton cannot be due to the spin forbidden nature of the $T_1 \rightarrow S_0$ transition. Both phosphorescent and thermally activated delayed fluorescent (TADF) materials, however, can harvest both singlet and triplet excitons to produce light but do so via distinct photophysical mechanisms. TADF materials have suitably small energy gaps between the S_1 and T_1 excited states (ΔE_{ST}) that enables triplet excitons to endothermically upconvert to singlets at ambient temperatures through a process called reverse inter-system crossing (RISC). The small ΔE_{ST} results from the small exchange integral where the HOMO and LUMO are localized on distinct parts of the emitter molecule. The most widely employed design is based on an an emitter with a strongly twisted donor-acceptor (D-A) conformation, where the HOMO will be mainly localized on the donor and the LUMO on the acceptor.

An archetype D-A TADF emitter is **DMAC-TRZ**, first reported by Tsai *et al*.[3] This compound has a very small ΔE_{ST} of 0.046 eV in 8 wt% doped films in mCPCN resulting from the near orthogonal conformation between the dimethylacridine (DMAC) donor and the triazine (TRZ) acceptor. In this host, **DMAC-TRZ** has a sky-blue emission with peak photoluminescence wavelength (λ_{PL}) of 495

nm and a high photoluminescence quantum yield (Φ_{PL}) of 90%. The OLEDs with this emitter showed a maximum external quantum efficiency, EQE_{max}, of 26.5% (at 1 cd m^{-2}), at a λ_{EL} of 500 nm. **DMAC-TRZ** also exhibits very low concentration quenching, with the neat film of the material having a Φ_{PL} of 83%; the non-doped device showed an EQE_{max} of 20.0%.[3] **DMAC-TRZ** has since been investigated extensively as the emitter in several computational and photophysical studies.[4–6]

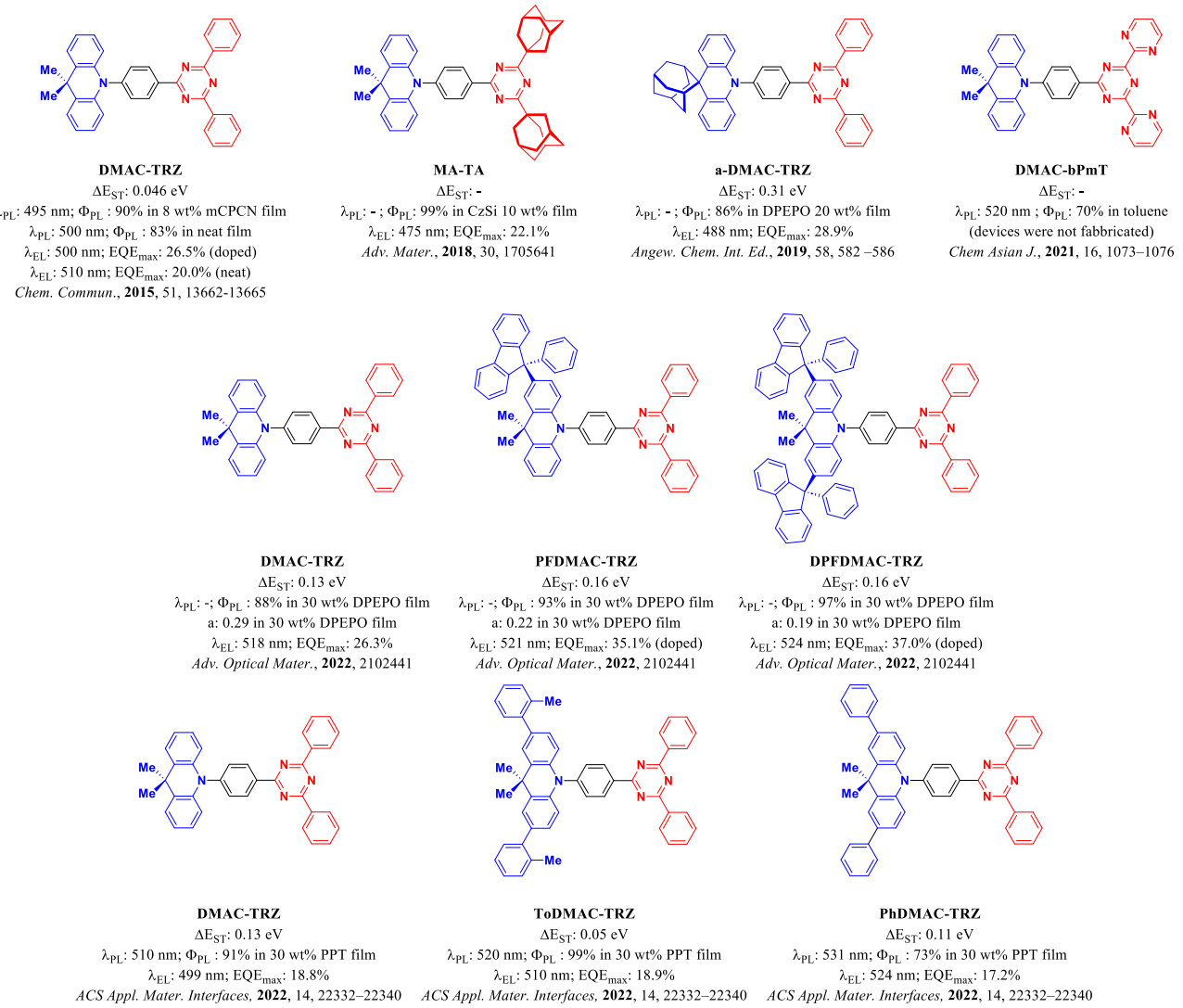

Figure **1**. Chemical structure and properties of **DMAC-TRZ** and several reported derivatives. The variation in reported ΔE_{ST} values of the doped films of **DMAC-TRZ** originates from a combination of the different doping concentration, host, and measurement parameters used in each study.

Many have focussed on improving further the molecular design of this emitter and have investigated derivatives. Kaji and co-workers reported two modified structures of **DMAC-TRZ** incorporating adamantane at different positions in **MA-TA**,[7] and **a-DMAC-TRZ**[8] (Figure **1**). In the first report, the substitution of the two distal phenyl rings on the triazine acceptor with adamantly groups reduced the

conjugation length of the acceptor, weakening it and leading to a bluer emission. Toluene solutions and neat films of **MA-TA** emit at 469 and 453 nm, respectively, compared to 494 and 500 nm for **DMAC-TRZ**. The 10 wt% doped film of **MA-TA** in CzSi shows a near unity Φ_{PL} of 99%, thus efficient solution-processed blue devices showed an EQE_{max} of 22.1%, at λ_{EL} of 475 nm.[9] The functionalization of the donor in **a-DMAC-TRZ** increased the rigidity of the structure ultimately leading to a more efficient device than with **DMAC-TRZ**, showing an EQE_{max} of 28.9% and a λ_{EL} of 488 nm.

Kaji and co-workers reported the emitter **DMAC-bPmT**, which contains two distal pyrimidines in lieu of phenyl groups in **DMAC-TRZ**.[10] The computational study revealed that the presence of these more π-accepting pyrimidines stabilize the energy of the S_2 and T_2 states, bringing them closer in energy to the S_1 and T_1 states, which enhanced the reverse intersystem crossing rate constant (k_{RISC}). Indeed, experimentally k_{RISC} is 8.8×10^5 s^{-1}, which is three times faster than the k_{RISC} of **DMAC-TRZ**, at 2.9×10^5 s^{-1}; however, the trade-off is that the Φ_{PL} of **DMAC-bPmT** of 70% is lower (Φ_{PL} of 93% for **DMAC-TRZ**) and the emission in toluene is red-shifted at λ_{PL} of 520 nm (λ_{PL} 500 nm for **DMAC-TRZ**).

Feng *et al.*[11] described an arylmethylation strategy to enhance the horizontal orientation of the transition dipole moment (TDM) of **DMAC-TRZ** derivatives in films. **PFDMAC-TRZ** and **DPFDMAC-TRZ** (Figure **1**) contain a functionalized DMAC donor containing one and two 9-phenyl-9H-fluorene groups, respectively. **PFDMAC-TRZ** and **DPFDMAC-TRZ** have the same ΔE_{ST} of 0.16 eV and high Φ_{PL} of 93 and 97%, respectively, in 30 wt% doped films in DPEPO. **DMAC-TRZ**, **PFDMAC-TRZ**, and **DPFDMAC-TRZ** possess anisotropy factors, *a*, of 0.29, 0.22, and 0.19, respectively, and the more horizontal orientation of the latter two was then exploited in the devices, which showed EQE_{max} of 26.3, 35.1, and 37.0%, respectively.[12]

ToDMAC-TRZ and **PhDMAC-TRZ** are examples of two other extended **DMAC-TRZ** derivatives (Figure **1**).[13] The functionalization of **DMAC-TRZ** with either *ortho*-tolyl unit and a phenyl unit results in a decreased ΔE_{ST} from 0.13 eV for **DMAC-TRZ** to 0.05 for **ToDMAC-TRZ** and 0.11 eV for **PhDMAC-TRZ,** in 30 wt% doped films in PPT. Although the ΔE_{ST} value of **DMAC-TRZ** here is different to the previously reported one,[3] likely a function of a combination of the different host, emitter concentration and measurement parameters used, in both cases the value is very small. The λ_{PL} in these doped films is red-shifted from 510 nm for **DMAC-TRZ** to 520 and 531 nm for **ToDMAC-TRZ** and **PhDMAC-TRZ**, respectively. This is due to the strengthening of the donor due to increased conjugation between these aromatic groups and the DMAC donor core. As 30 wt% doped

films in PPT, **DMAC-TRZ**, **ToDMAC-TRZ**, and **PhDMAC-TRZ** have Φ_{PL} of 91, 99, and 73%, respectively. The trend in EQE_{max} of 18.8, 18.9, and 17.2% of the corresponding devices mirrors their Φ_{PL} while their λ_{EL} are blue-shifted at 499 nm, 510 nm, and 524 nm, respectively, compared to their λ_{PL}. Despite the lower efficiency, the OLED with **PhDMAC-TRZ** possessed a much longer lifetime (LT_{50} of 1910 h) than that with **DMAC-TRZ** (LT_{50} of 70 h); the OLED with **ToDMAC-TRZ** also showed an improved lifetime, but only at 198 h.

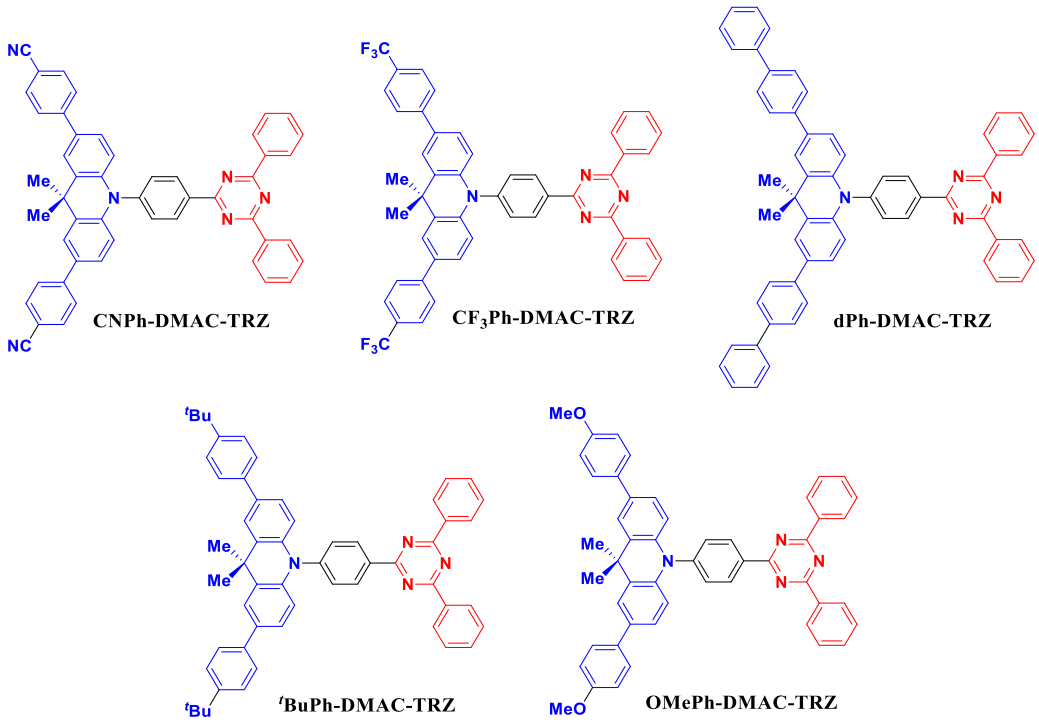

Figure **2**. Chemical structure of **CNPh-DMAC-TRZ**, **CF_3Ph-DMAC-TRZ**, **dPh-DMAC-TRZ**, **^{t}BuPh-DMAC-TRZ, OMePh-DMAC-TRZ**.

Here, we report a rationally designed family of **DMAC-TRZ** derivatives, **CNPh-DMAC-TRZ**, **CF_3Ph-DMAC-TRZ**, **dPh-DMAC-TRZ**, **^{t}BuPh-DMAC-TRZ, MeOPh-DMAC-TRZ** (Figure **2**) wherein the central DMAC donor is decorated with two aryl groups containing at the 4-position differing electron-donating or withdrawing groups. The effect of donor decoration on the colour tuning of the emitters, their triplet exciton harvesting, and PL efficiencies is demonstrated. Further, using angle resolved photoluminescence spectroscopy we explore how the increased molecular weight and length of the emitter (depending on the nature of the peripheral substituent on the donor), affects the orientation of its TDM. Using light outcoupling simulations, the effect of TDM orientation on the light outcoupling efficiency is explored, showing a small improvement in outcoupling efficiency in most cases, compared to **DMAC-TRZ**.

Results and discussion

Theoretical calculations

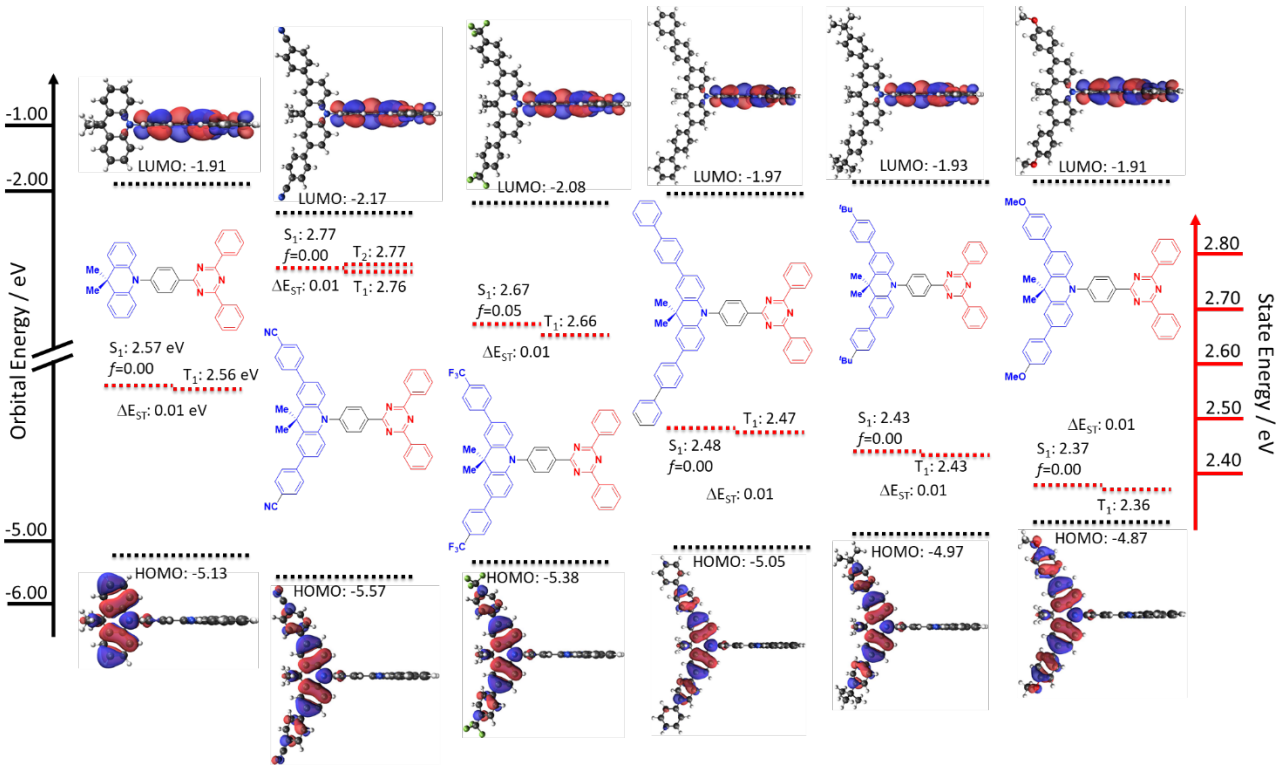

Figure **3.** HOMO and LUMO electron density distributions and energy levels, excited-state energy levels of **DMAC-TRZ** and its five derivatives (Obtained via DFT and TD-DFT at the PBE0/6-31G(d,p) level, Isovalues: MO=0.02, Density=0.0004).

The optoelectronic properties of **DMAC-TRZ** and the five new derivatives were first assessed using a combined DFT and TD-DFT theoretical study at the PBE0/6-031G(d,p)[14,15] level (Figure **3**). **DMAC-TRZ** has HOMO and LUMO energy levels of -5.13 eV, and -1.91 eV, respectively. The DMAC is twisted to almost 90° with respect to the triazine, as previously observed in the literature,[3] leading to a very small overlap between the HOMO located on the DMAC and the LUMO located on the triazine, and thus an almost zero ΔE_{ST}; S_1 and T_1 levels are 2.57 eV and 2.56 eV, respectively. The small overlap between the HOMO and LUMO also leads to an oscillator strength with a value of zero.

The ground-state optimized structures of the five derivatives all possess similar conformations as that of **DMAC-TRZ**, thus leading to ΔE_{ST} values of ca. 0.01 eV. As the substituents at the 4-position of the aryl groups change from electron-withdrawing (CN and CF_3) to electron-donating (^{t}Bu and OMe) the HOMO energy level becomes progressively destabilized, with values of -5.57, -5.38, -5.05, -4.97,

and -4.87 eV for **CNPh-DMAC-TRZ**, **CF_3Ph-DMAC-TRZ**, **dPh-DMAC-TRZ**, **^{t}BuPh-DMAC-TRZ**, **OMePh-DMAC-TRZ**, respectively. The LUMO levels are likewise destabilized along the series though to a lesser extent than the HOMO levels as the triazine is only weakly conjugated to the DMAC-based donor. The LUMO values are -2.17, -2.08, -1.97, -1.93, and -1.91 eV for **CNPh-DMAC-TRZ**, **CF_3Ph-DMAC-TRZ**, **dPh-DMAC-TRZ**, **^{t}BuPh-DMAC-TRZ**, **OMePh-DMAC-TRZ**, respectively. The HOMO level of **DMAC-TRZ** (-5.13 eV) falls in the middle of the series between **CF_3Ph-DMAC-TRZ** and **dPh-DMAC-TRZ**. The LUMO of **DMAC-TRZ** (-1.91 eV) falls between those of **dPh-DMAC-TRZ** and **^{t}BuPh-DMAC-TRZ**. The biphenyl group is an inductively electron-withdrawing moiety, which can then slightly stabilize the LUMO level, making it lower in energy than **DMAC-TRZ**.

The singlet and triplet energy levels are also affected by the nature of the substituent on the DMAC donor. The energies of the excited states become systematically more stabilized across the series (Figure **3**). The S_1/T_1 energies are 2.77/2.76, 2.67/2.66, 2.48/2.47, 2.37/2.36, and 2.43/2.43 eV for **CNPh-DMAC-TRZ**, **CF_3Ph-DMAC-TRZ**, **dPh-DMAC-TRZ**, **^{t}BuPh-DMAC-TRZ**, **OMePh-DMAC-TRZ**, respectively. The S_1/T_1 energies of **DMAC-TRZ** lie between those of **CF_3Ph-DMAC-TRZ** and **dPh-DMAC-TRZ**. All the compounds possess S_1 and T_1 states that possess charge transfer (CT) character (HOMO→LUMO transition). **dCNPh-DMAC-TRZ** is the only molecule that has a degenerate T_2 state, which has a locally-excited (LE) character, localized on the donor moiety (HOMO→LUMO+2 transition). The c.a. 90° conformation, and very small ΔE_{ST} values of ca. 0.01 eV also leads to an effective oscillator strength value of 0.00. The only exception is observed in **CF_3Ph-DMAC-TRZ** with a *f* of 0.05.

Synthesis

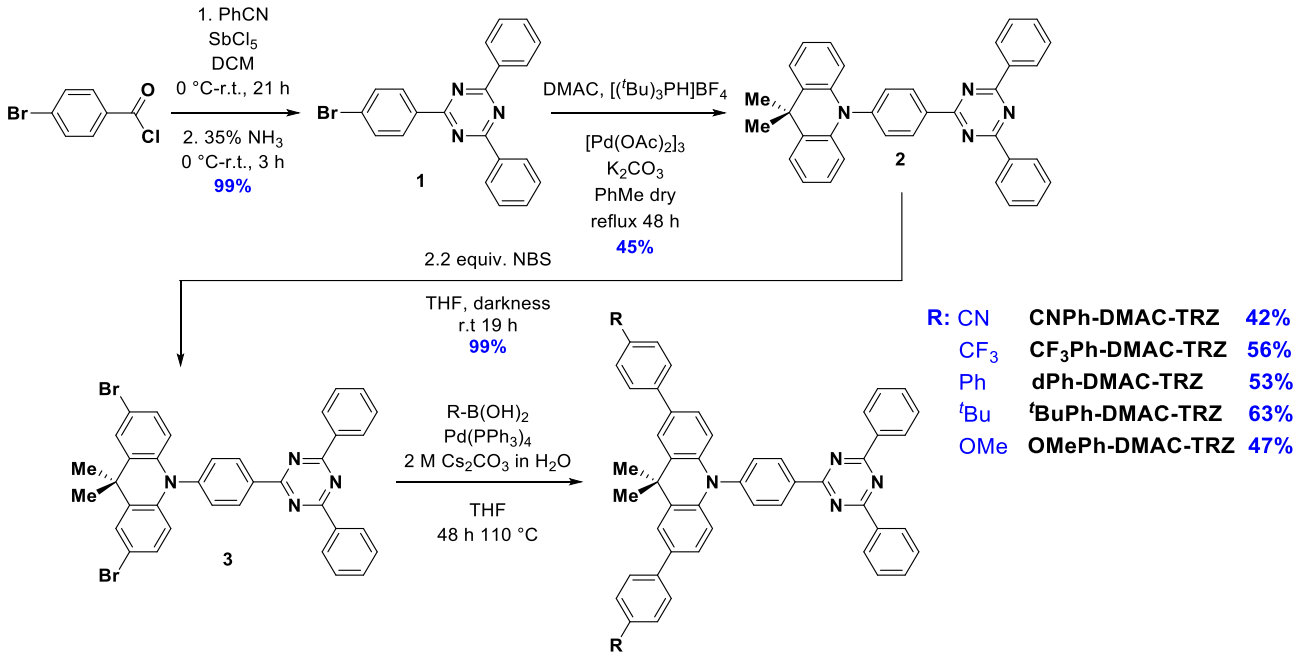

Scheme **1**. Synthetic procedure for the five **DMAC-TRZ** derivatives.

The five **DMAC-TRZ** derivatives were synthesized *via* a four-step synthetic procedure (Scheme **1**). Bromotriazine (**1**)was obtained in quantitative yield following a Lewis acid-catalyzed cyclization of 4-bromobenzoyl chloride and benzonitrile using antimony pentachloride in DCM, followed by the addition of 35% ammonia.[16] The triazine is then coupled to DMAC through a Buchwald-Hartwig coupling in 40% yield.[3] **DMAC-TRZ** (**2**) was then quantitatively dibrominated using 2.2 equivalents of NBS in THF, shielded from light.[17] Finally, the DMAC-TRZ derivatives were accessed via a Suzuki-Miyaura cross-coupling of **3** with the corresponding aryl-boronic acid, the reaction was carried out in a pressure vessel at 110 °C for 48 h to improved the yield of the coupled products. Yields for the final step ranged between c.a. 42 and 63%. The identity and purity of the compounds were confirmed by a combination ^{1}H, ^{13}C, and ^{19}F NMR spectroscopy, Mp determination, HRMS, HPLC, and EA.

Optoelectronics properties

CV and DPV of **DMAC-TRZ** (for comparison) and the five emitters (Figure **4a**) were carried out in DCM. The electrochemistry of **DMAC-TRZ** (oxidation attributed to the DMAC and reduction attributed to the triazine) matches that previously reported data,[3,18,19] with oxidation and reduction potentials at E_{ox} of 0.97 V and E_{ox} red -1.72 V, respectively (taken from DPV) versus SCE. The corresponding HOMO and LUMO energy values are -5.31 V and -2.62 V, respectively.

Despite the predicted small changes in LUMO energies, there is no significant change in the reduction potentials, with values of -1.68, -1.68, -1.69, -1.71, and -1.69 V for **CNPh-DMAC-TRZ**, **CF_3Ph-DMAC-TRZ**, **dPh-DMAC-TRZ**, **^{t}BuPh-DMAC-TRZ**, **OMePh-DMAC-TRZ**, respectively, leading to LUMO values of around ~ -2.65 eV, comparable to that of **DMAC-TRZ** (-2.62 eV). The oxidation potentials follow the trend observed for the DFT calculations, with electron-donating and conjugating groups cathodically shifting the oxidation potential, with values of 1.04, 1.01, 0.87, 0.81, and 0.79 V for **CNPh-DMAC-TRZ**, **CF_3Ph-DMAC-TRZ**, **dPh-DMAC-TRZ**, **^{t}BuPh-DMAC-TRZ**, **OMePh-DMAC-TRZ**, respectively. The HOMO energy levels values, obtained from these measured oxidation potentials, are -5.38, -5.35, -5.21, -5.15, and -5.13 eV for **CNPh-DMAC-TRZ**, **CF_3Ph-DMAC-TRZ**, **dPh-DMAC-TRZ**, **^{t}BuPh-DMAC-TRZ**, **OMePh-DMAC-TRZ**, respectively, while **DMAC-TRZ** falls in the middle of the series (-5.31 eV).

The UV-vis absorption of **DMAC-TRZ** and its five derivatives were carried out in a toluene solution (Figure **4**Error! Reference source not found.**b, c**). The very low intensity of the lowest energy absorption band of **DMAC-TRZ** (~ 400 nm) is reflective of the orthogonal conformation between donor and acceptor. In this conformation, the poor overlap between HOMO and LUMO results in an oscillator strength of almost zero, reflected in the very low molar absorptivity for this CT transition (ε value of 2000 $M^{-1}cm^{-1}$).

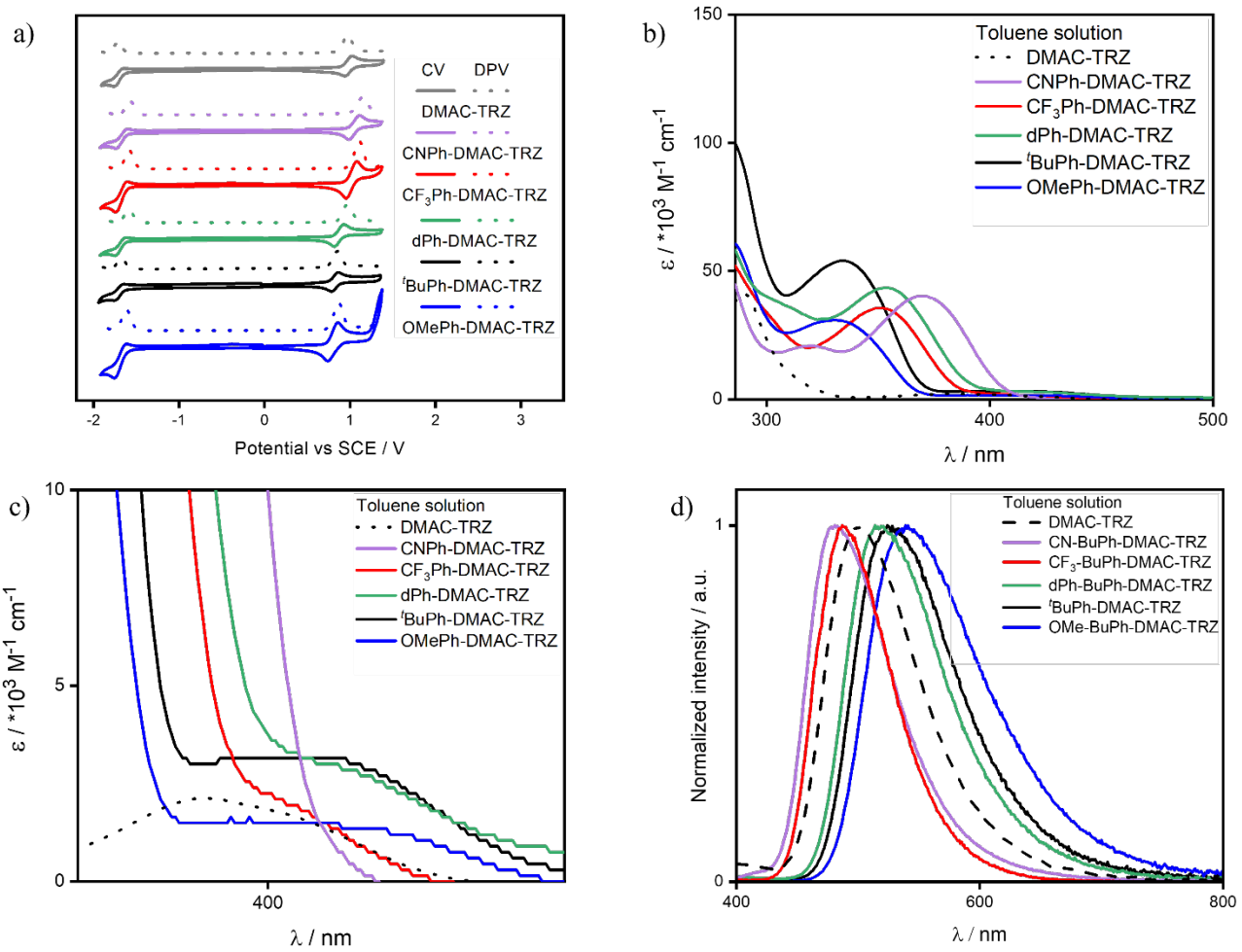

Figure **4.** a) Cyclic Voltammetry (CV) and Differential Pulse Voltammetry (DPV) of **DMAC-TRZ** and derivatives in DCM (scan rate = 100 mV/s); b) UV-vis absorption spectra of **DMAC-TRZ**, and derivatives in toluene and c) zoom on the low intensity CT bands; d) Photoluminescence spectra of **DMAC-TRZ** and its derivatives in toluene (λ_{exc}= 340 nm).

The absorption spectra of the five derivatives reveal the first instance of a structure-property trend that will be a staple for the series: **^{t}BuPh-DMAC-TRZ** and **OMePh-DMAC-TRZ** have similar behaviour, as do **CF$_3$Ph-DMAC-TRZ**, and **dPh-DMAC-TRZ**, while the behaviour of **CNPh-DMAC-TRZ** is rather distinct. Distinct from the absorption spectrum of **DMAC-TRZ,** there is a well-defined low-energy band ($\varepsilon > 10^4$ M^{-1}cm^{-1}) in the absorption spectra of all five emitters (Figure **4b**). This band is assigned to a π–π* transition localized on the aryl-substituted DMAC donors.[10] The donor-acceptor CT absorption bands of the five derivatives, characterised by their low energy and small extinction coefficient, are shown in Figure **4c**. The CT absorption band falls around 410 nm for **^{t}BuPh-DMAC-TRZ**, **dPh-DMAC-TRZ** and **OMePh-DMAC-TRZ**, with ε values of 3050, 3040, and 1190 M^{-1}cm^{-1}, respectively. The CT band is slightly blue-shifted in **CF$_3$Ph-DMAC-TRZ** at

around 400 nm (ε = 2170 $M^{-1}cm^{-1}$) and is of a similar profile to that of the highly twisted conformer of **DMAC-TRZ**. **CNPh-DMAC-TRZ** has two absorption bands, at 369 nm and 318 nm, assigned by TDDFT calculations (Figure **S35**) to different ^{1}LE transitions on the acridine donor to the S_3, and S_5 states, respectively, with ε values of 40,150 M^{-1} cm^{-1} (at 369 nm) and 20,330 M^{-1} cm^{-1} (at 318 nm). The red-shifted strong absorption bands of the CNPh-acridine donor obscures the weak ^{1}CT absorption.

The absorption and emission spectra of **DMAC-TRZ** and its five derivates were measured in different polarity solvents (Figure **S36**). The absorption spectra are mostly unaffected by the solvent polarity, presumably because of the low ground-state dipole moment of these compounds, while the emission spectra follow the expected bathochromic shift with increasing solvent polarity that is associated with excited states of CT character. Indeed, toluene, THF, and DCM solutions show broad and unstructured spectra, typical of a CT-type emission, while methyl-cyclohexane shows a narrower and more structured LE-type emission, in all cases.

The photophysics of the emitters were then investigated in degassed toluene solution (Figure **S37**). **DMAC-TRZ** in toluene emits at 500 nm. **CNPh-DMAC-TRZ**, and **CF_3Ph-DMAC-TRZ** present blue-shifted emission (λ_{PL} of 484 and 487 nm, respectively), while the other derivatives emission is red-shifted (λ_{PL} of 511, 518, and 528 nm for **dPh-DMAC-TRZ**, **^{t}BuPh-DMAC-TRZ**, and **OMePh-DMAC-TRZ**, respectively), compared to **DMAC-TRZ** (Figure **4d)**. **DMAC-TRZ** in degassed toluene solution has a Φ_{PL} of 67%, which decreases to 21% when exposed to air. This is lower than the literature reported value (Φ_{PL} ~ 93%), presumably due to different excitation wavelength used and measurement method.[10] **CNPh-DMAC-TRZ**, **CF_3Ph-DMAC-TRZ**, **dPh-DMAC-TRZ**, **^{t}BuPh-DMAC-TRZ**, **OMePh-DMAC-TRZ** have Φ_{PL} values (degassed/aerated) of 41/32%, 72/28%, 70/35%, 74/24%, and 75/23%, respectively. Thus, all compounds have larger Φ_{PL} compared to the parent emitter, apart from **CNPh-DMAC-TRZ**, which also shows less sensitivity to oxygen quenching. To explore the latter, and more specifically the contribution of the delayed component, time-resolved photoluminescence measurements (TRPL) were carried out in both the degassed and aerated toluene solutions.

The TRPL of the degassed toluene solution of **DMAC-TRZ** possesses both prompt and delayed components with mono-exponential decays and lifetimes, τ_p, of 20.8 ns and τ_d, of 5.21 μs, respectively (**Error! Reference source not found.**). These lifetimes are comparable to those previously reported in the literature for the same compound.[5] As expected, the delayed component disappears after the solution is exposed to air. The derivatives decorated with electron-donating

groups have slightly longer τ_p than **DMAC-TRZ**, with mono-exponential decays of 28.70 ns and 28.09 ns for **^{t}BuPh-DMAC-TRZ** and **OMePh-DMAC-TRZ**, respectively (Figure **S37**). Their degassed solutions possess much shorter delayed lifetimes than **DMAC-TRZ**, with mono-exponential τ_d of 2.39 μs, and 1.49 μs, for **^{t}BuPh-DMAC-TRZ** and **OMePh-DMAC-TRZ**, respectively, which each disappear when the solution is exposed to air. This implies a more efficient reverse intersystem crossing rate (k_{RISC}) for these two emitters, as both the amplitude and lifetime of the delayed component improves. The TRPL of **CF_3Ph-DMAC-TRZ** and **dPh-DMAC-TRZ** appears to behave in the opposite manner with shorter τ_p of 10.9 ns and 15.4 ns, respectively (Figure **S37**) and longer τ_d and biexponential decay kinetics (average τ_d of 20.7 μs and 25.8 μs, respectively), which also disappear after exposure to air. There is no delayed emission observed for **CNPh-DMAC-TRZ** and the τ_p is 8.24 ns, which decreases to 6.53 ns when exposed to air due to a small degree of singlet quenching caused by the presence of oxygen.[20] The short prompt lifetime is consistent with emission from a LE state.

The photophysical properties of the materials in solid-state were first studied in the host matrix mCP (Figure **S38**). This host was chosen as it has a relatively high triplet energy (2.9 eV), which makes it suitable for both green and blue devices.[21] The Φ_{PL} of **^{t}BuPh-DMAC-TRZ** appears to decrease slightly at concentrations above 10 wt% (Table **6**). Thus, 10 wt% loading was chosen for all the emitters in mCP.[5] The trend in the solid-state PL spectra of the six emitters at 10 wt% in mCP (Figure **S38a**) matches that observed in toluene (Figure **8d**). Interestingly, the λ_{PL} of **DMAC-TRZ**, **CNPh-DMAC-TRZ** and **CF_3Ph-DMAC-TRZ** are almost isoenergetic in mCP (Table **S5**). This is attributed to the stronger intermolecular interactions taking place in the films.[22,23]

The TRPL behaviour in the mCP films is also comparable to that observed in toluene; notably, there is a small degree of delayed emission observed for **CNPh-DMAC-TRZ** (**Error! Reference source not found.S38**). The presence of electron-donating substituents on the donor leads to a longer-lived prompt fluorescence, while the opposite trend is the observed for the delayed fluorescence lifetimes. The TADF character of all the materials was confirmed by temperature dependent TRPL measurements, where the contribution from the delayed emission increases with increasing temperature (Figure **S38**). The delayed emission of both **^{t}BuPh-DMAC-TRZ** and **OMePh-DMAC-TRZ** is only modestly quenched at 80 K, attributed to the highly efficient RISC process in these two emitters, thus at this temperature triplet harvesting is not fully suppressed.[24] This effect is also observed for their 80 K temperature phosphorescence spectra, which are not structured, resulting to a misleading triplet energy value, while their 20 K phosphorescence spectra are more structured (indicating mixed CT/LE character) and the triplet energy value appears similar in both molecules,

around 2.65 eV (Figure **S39**). This results in a ΔE_{ST} of 30 meV for both emitters and is in good agreement with the DFT calculations (Figure **3**). For **CNPh-DMAC-TRZ**, **CF$_3$Ph-DMAC-TRZ**, and **dPh-DMAC-TRZ**, 80 K is a sufficiently low temperature to effectively suppress TADF, and structured phosphorescence is observed with energy onset at 2.5, 2.63, and 2.54 eV, respectively (Figure **S39**). The resulting ΔE_{ST} values are 290, 210, and 150 meV for **CNPh-DMAC-TRZ**, **CF$_3$Ph-DMAC-TRZ**, and **dPh-DMAC-TRZ**, respectively (Table **1**). From the modelled lowest triplet value of the aryl decorated donor units (Figure **S40**), **CNPh-DMAC**, **CF$_3$Ph-DMAC**, and **dPh-DMAC** have more stabilized T_1 states compared to **^{t}BuPh-DMAC** and **OmePh-DMAC**, these trend in a similar manner to the experimentally obtained values. Consequently, we propose that in **CNPh-DMAC-TRZ**, **CF$_3$Ph-DMAC-TRZ**, and **dPh-DMAC-TRZ** the T_1 state is localized on the aryl-decorated acridine donor, while in **^{t}BuPh-DMAC-TRZ** and **OMePh-DMAC-TRZ** T_1 state has a mixed CT/LE character.

The Φ_{PL} of the six emitters in 10 wt% mCP are compiled in Table **S5**. In all cases, the Φ_{PL} of the mCP films is lower than in toluene. It has already been established that the Φ_{PL} of **DMAC-TRZ** is higher in higher dipole moment matrices.[3] For these reasons a screening of the Φ_{PL} in high triplet energy hosts mCP, mCBPCN and DPEPO host was conducted using **^{t}BuPh-DMAC-TRZ** as a representative example (Table **S6**). As well, mCBPCN and DPEPO have high MW and T_g, which would be beneficial to influence the horizontal orientation of the TDM of these materials.[12] At concentrations below 10 wt% the Φ_{PL} values are similar in the three hosts, because the measurement error is higher.[5] At higher concentrations, the Φ_{PL} values in mCBPCN and DPEPO are similar and higher than those in mCP. Thus, mCBPCN was chosen as the host material to carry on the solid-state photophysical analysis, as DPEPO is recognized to be unstable in the OLEDs and this would thus negatively impact the device lifetime.[25] Further, 10 wt% was chosen as the doping concentration as at this concentration there are few intermolecular interactions as already observed in films of **DMAC-TRZ**.[5,26] The Φ_{PL} values in 10 wt% mCBPCN are 87, 34, 70, 70, 72, and 72% for **DMAC-TRZ, CNPh-DMAC-TRZ**, **CF$_3$Ph-DMAC-TRZ**, **dPh-DMAC-TRZ**, **^{t}BuPh-DMAC-TRZ**, and **OMePh-DMAC-TRZ**, respectively (Table **S5**).

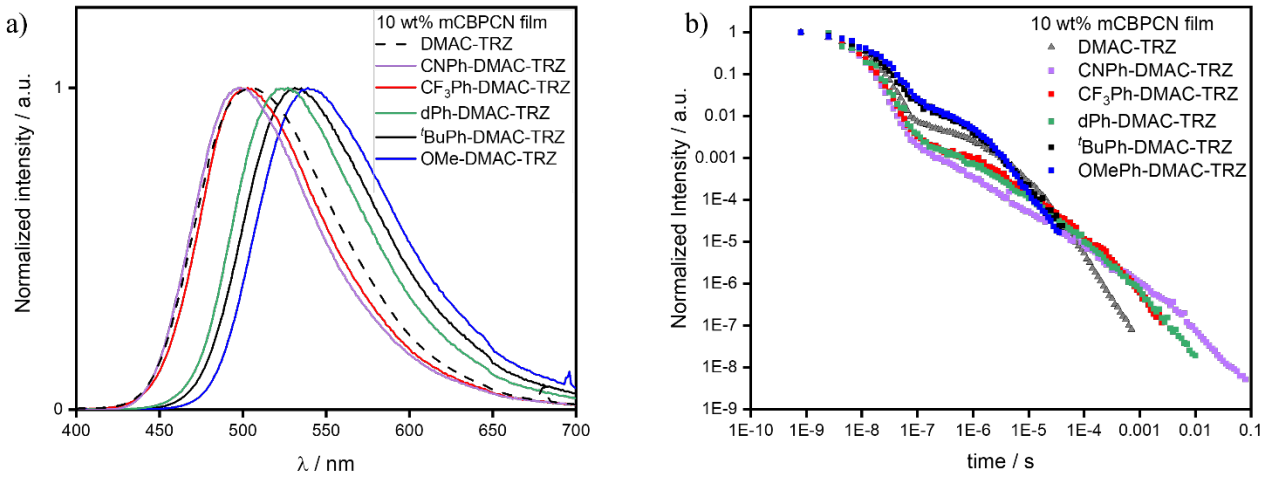

Figure **5**. a) Photoluminescence spectra and b) time-resolved emission decays at room temperature of **DMAC-TRZ** and its five derivatives in 10 wt% doped films in mCBPCN (λ_{exc}= 355 nm).

The 10 wt% doped films in mCBPCN of **DMAC-TRZ**, **CNPh-DMAC-TRZ**, **CF$_3$Ph-DMAC-TRZ**, **dPh-DMAC-TRZ**, **^{t}BuPh-DMAC-TRZ**, **OMePh-DMAC-TRZ** emit at λ_{PL} of 505 nm, 498 nm, 503 nm, 527 nm, 531 nm, 539 nm, respectively (Figure **5a)**. The emission spectra of **^{t}BuPh-DMAC-TRZ**, **OMePh-DMAC-TRZ** and **dPh-DMAC-TRZ** are red-shifted compared to the ones in 10 wt% mCP films, while the spectra of **CF$_3$Ph-DMAC-TRZ** and **CNPh-DMAC-TRZ** do not change much (Table **S5**). The average room temperature τ_p are 7.8 ns, 9.5 ns, 10.5 ns, 16.2 ns, and 18.5 ns for **CNPh-DMAC-TRZ**, **CF$_3$Ph-DMAC-TRZ**, **dPh-DMAC-TRZ**, **^{t}BuPh-DMAC-TRZ**, and **OMePh-DMAC-TRZ**, respectively (Table **1**). As was observed in both solution and in mCP films, longer-lived prompt fluorescence is observed when the DMAC contains electron-donating substituents. The magnitude of the delayed component is similar to that of the doped mCP films for all emitters except **^{t}BuPh-DMAC-TRZ** and **OMePh-DMAC-TRZ**, which have higher DF contribution in their decay profile. The average τ_d is 1.2 ms, 163, 305, 2.64, and 1.99 µs for **CNPh-DMAC-TRZ**, **CF$_3$Ph-DMAC-TRZ**, **dPh-DMAC-TRZ**, **^{t}BuPh-DMAC-TRZ**, and **OMePh-DMAC-TRZ**, respectively (Table **1**). These lifetimes also follow the same trend as previously discussed for toluene where the delayed lifetimes become shorter in emitters containing more electron-rich donors. **DMAC-TRZ** was measured in the same environment as a comparison, showing lifetimes that are intermediate, with an average τ_p and τ_d of 12.1 ns and 15.6 µs, respectively.

The decay kinetics were calculated following the method of Tsuchiya *et al.* (Table **1**).[20] All materials possess k_F and a k_{ISC} of the order of $10^7 - 10^8$ s^{-1}. The k_{RISC} were estimated to be 9.2 × 10^5 s^{-1} and 7.8 × 10^5 s^{-1} for **^{t}BuPh-DMAC-TRZ** and **OMePh-DMAC-TRZ**, respectively. These rates are four times

faster compared to that of **DMAC-TRZ** (k_{RISC} = 2.2 × 10^5 s^{-1}), and one order of magnitude faster than the k_{RISC} of **CF_3Ph-DMAC-TRZ**, **dPh-DMAC-TRZ**; the slowest k_{RISC} was observed for **CNPh-DMAC-TRZ** (Table **1**). The trend in estimated k_{RISC} values aligns well with the relative magnitude of the ΔE_{ST} (Figure **S39**).

Table **1**. Kinetics analysis[20] of 10 wt% doped films of **DMAC-TRZ** and its five derivatives in mCBPCN.

R-DMAC-TRZ	Φ_{PL} N_2 (%)	A_{PF} (a.u.)	$\tau_{PF\ avg}$[a] (× 10^{-9} s)	A_{DF} (× 10^{-4} a.u.)	$\tau_{DF\ avg.}$[a] (× 10^{-6} s)	Φ_{PL}[b] (%)	Φ_{PF}[c] (%)	Φ_{DE}[c] (%)	$k_{F\ avg.}$[a] (× 10^7 s^{-1})	$k_{ISC\ avg.}$[a] (× 10^7 s^{-1})	$k_{RISC\ avg.}$[a] (× 10^5 s^{-1})
^{t}BuPh-	72	0.88	16.2	66.1	2.64	72	32.6	39.4	6.19	4.69	7.59
OMePh-	72	0.87	18.5	92.6	1.99	72	34	38.1	5.41	3.99	9.59
dPh-	70	0.96	10.5	0.29	305	70	37.5	32.5	9.52	6.37	0.05
CF_3Ph-	70	0.98	9.5	0.64	163	70	33	37	10.5	7.71	0.12
CNPh-	34	0.95	7.8	0.06	1220	34	17	17	12.8	6.83	0.01
H-	87	0.89	12.1	9.87	15.6	87	35.8	51.2	8.30	7.08	1.49

[a] Average values were extracted from the averaging of the multiple exponentials used to fit the prompt and delayed lifetimes using the following equation:

$$\tau_{avg.} = \sum_{i=1}^{n}(A_i{\tau_i}^2)/\sum_{i=1}^{n}(A_i\tau_i)$$

[b] Obtained using an integrating sphere, under a nitrogen atmosphere, λ_{exc} = 340 nm.

[c] Obtained from the integrated prompt and delayed emission of the TRPL decays.[27]

Orientation measurements

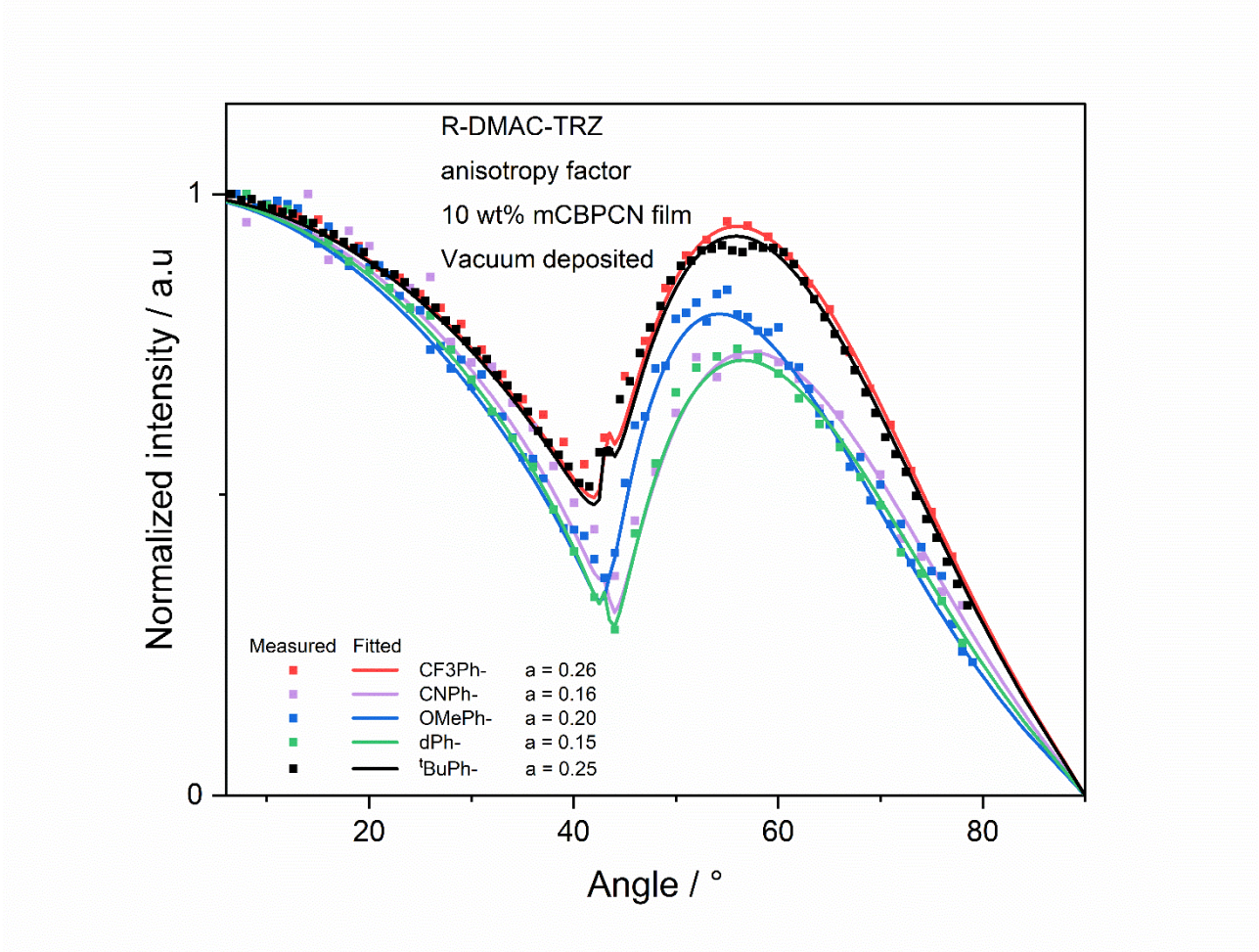

Figure **6**. Angle-resolved photoluminescence measurement of **CNPh-DMAC-TRZ**, **CF_3Ph-DMAC-TRZ**, **dPh-DMAC-TRZ**, **^{t}BuPh-DMAC-TRZ**, **OMePh-DMAC-TRZ** in evaporated 10 wt% doped films in mCBPCN. The dotted line shows the measurement, and the continuous line of the matching color shows a fit using the dipole emission model, yielding the anisotropy factor, *a* (data taken at λ_{PL}= 490 nm, 500 nm, 520 nm, 521 nm, and 539 nm for **CNPh-DMAC-TRZ**, **CF_3Ph-DMAC-TRZ**, **dPh-DMAC-TRZ**, **^{t}BuPh-DMAC-TRZ**, **OMePh-DMAC-TRZ**, respectively).

The orientation of the transition dipole moment (TDM) of the series of derivatives was measured in evaporated 10 wt% doped films in mCBPCN (Figure **6**, Table **14**). All materials exhibit a preferential horizontal orientation of their TDM, with *a* values of 0.16, 0.26, 0.15, 0.25, and 0.20 for **CNPh-DMAC-TRZ**, **CF_3Ph-DMAC-TRZ**, **dPh-DMAC-TRZ**, **^{t}BuPh-DMAC-TRZ**, **OmePh-DMAC-TRZ**, respectively. The *a* value of **DMAC-TRZ** in the same environment of 0.21 lies in between those of the five derivatives.[4] As previously mentioned, Tenopala *et al.*[12] found that generally for emitters with MW> 600 g/mol, the anisotropy factor improves with higher MW, higher x_E/x_H (ratio of the length of the emitter to the host), and lower z_E (thickness of the emitter)[12] (Table **S7**). All five derivatives (as well as the parent compound **DMAC-TRZ**) have the same z_E value, thus it will not be

considered in this analysis. The orthogonal conformation of the material means that the donor is responsible for the width of the material (y_E) and the thickness of the material is dependent on the triazine, which is the same in all materials. The material with the lowest *a* value is **dPh-DMAC-TRZ**, which can be rationalized as it is the heaviest material (MW of 821.02 g/mol) and has the highest x_E/x_H value of the series (x_E/x_H = 1.35). However, the material with the second lowest *a* value is **CNPh-DMAC-TRZ**, which is the lightest material (MW of 718.84 g/mol) and has the smallest x_E/x_H value of the series (x_E/x_H = 1.08). The other materials classify, in increasing *a*, are **OmePh-DMAC-TRZ** (*a* = 0.19), **^{t}BuPh-DMAC-TRZ** (*a* = 0.25), and **CF_3Ph-DMAC-TRZ** (*a* = 0.26); no discernable trend was identified for these materials. Furthermore, **DMAC-TRZ** (MW = 516.63 g/mol) is even lighter than all its derivatives, but still has an appreciable orientation factor (*a* = 0.21). Thus, the simple geometrical arguments do not apply here.

Table **1**. Orientation data of the five derivatives obtained from angle-resolved photoluminescence measurements in evaporated 10 wt% doped films mCBPCN.

Emitter	***a*[a]**	**θ_h[b]**	**S[c]**
CNPh-DMAC-TRZ	0.16	0.84	-0.275
CF_3Ph-DMAC-TRZ	0.26	0.74	-0.11
dPh-DMAC-TRZ	0.15	0.85	-0.29
^{t}BuPh-DMAC-TRZ	0.25	0.75	-0.13
OmePh-DMAC-TRZ	0.20	0.80	-0.22
DMAC-TRZ	0.21	0.79	-0.19

[a] anisotropy factor; [b] fraction of horizontal dipole (θ_h = 1-*a*); [c] orientation order parameter (S = (3*a*-1)/2.

OLEDs

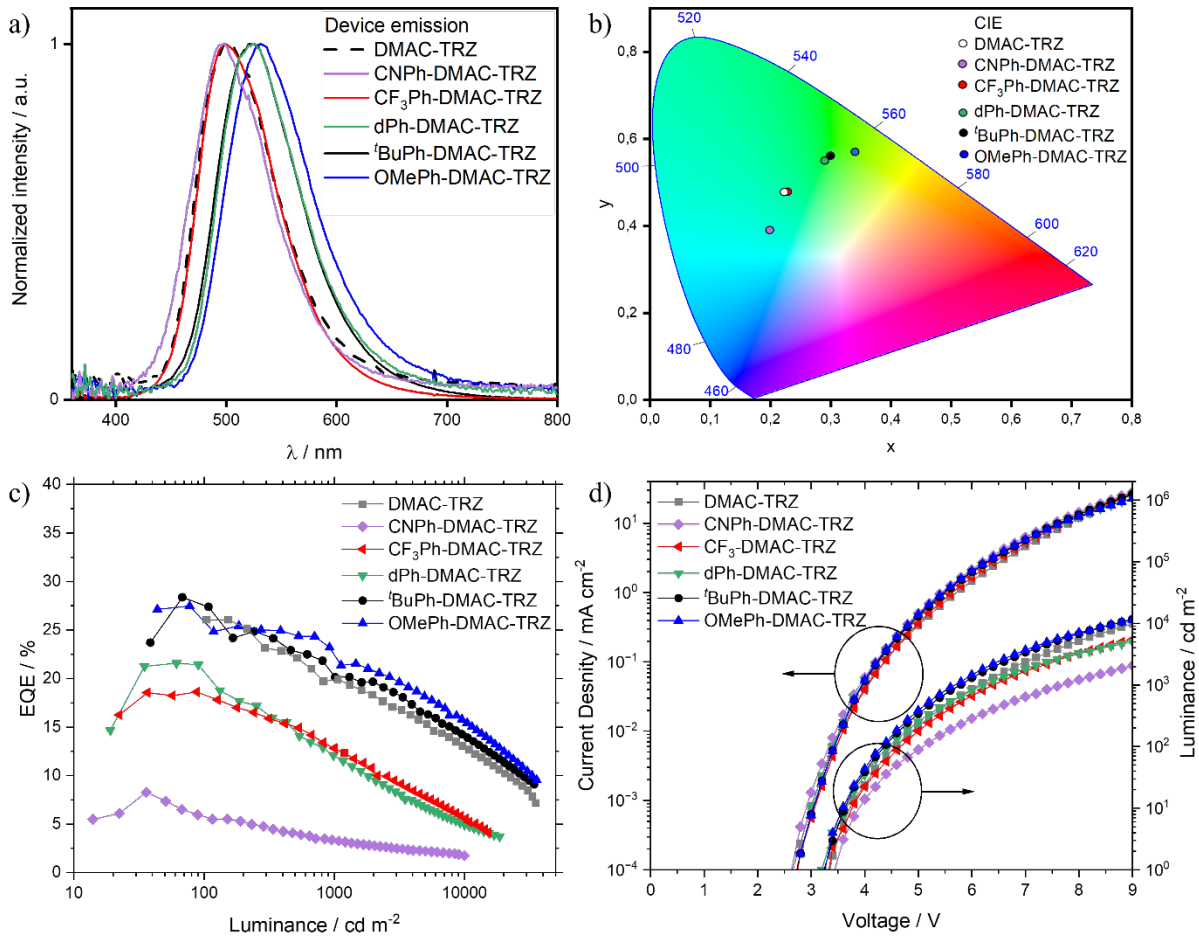

Figure 7. a) Electroluminescence spectra (at 1000 cd m^{-2}) of **CNPh-DMAC-TRZ**, **CF_3Ph-DMAC-TRZ**, **dPh-DMAC-TRZ**, **^{t}BuPh-DMAC-TRZ**, **OmePh-DMAC-TRZ** 10 wt% doped in mCBPCN; b) CIE coordinates of the devices (the CIE coordinates of the devices with **DMAC-TRZ** and **CF_3Ph-DMAC-TRZ** are identical, precisely under the white dot); c) EQE vs Luminance curves of the OLEDs with **DMAC-TRZ** and its derivatives; d) Current density vs Current vs Luminance curves of the OLEDs.

OLEDs were fabricated with the following architecture: ITO/NPB (35 nm)/NPB:mCBP 1:1 (5 nm)/mCBP (10 nm)/mCBPCN:**R-DMAC-TRZ** x wt% (30 nm)/T2T (10 nm)/T2T:LiQ 1:1 (35 nm)/LiQ (1 nm)/Al (100 nm) (**Error! Reference source not found.1**). Initially, OLEDs of **^{t}BuPh-DMAC-TRZ** at different doping concentrations were fabricated (Figure **S42**). While the efficiency roll-off improves at higher emitter doping concentrations, the overall efficiency significantly decreases with increasing emitter doping, from 10 wt% to the non-doped device, with an EQE_{max} of 28, 21, 18.6, 11.8, and 6.1% for the devices with 10, 20, 30, 60 wt% doping and non-doped device, respectively. From the 10 wt% to the non-doped device, a red-shift of c.a. 10 nm is observed. Thus, OLEDs of the five derivatives, at 10 wt% concentration, were fabricated.

The performance of the OLEDs is summarized in Table **2**. All devices have similar turn-on voltage between 3.2 - 3.4 V, and the electroluminescence maxima (λ_{EL}) followed the same trend observed in the thin film SSPL (**Error! Reference source not found.**a). The λ_{EL} was 501, 496, 498, 525, 526, and 531 nm for the **DMAC-TRZ**, **CNPh-DMAC-TRZ**, **CF_3Ph-DMAC-TRZ**, **dPh-DMAC-TRZ**, **^{t}BuPh-DMAC-TRZ**, and **OMePh-DMAC-TRZ** OLEDs, respectively.

The **^{t}BuPh-DMAC-TRZ** and **OMePh-DMAC-TRZ** devices showed the highest EQE_{max} of 28 and 27.4%, respectively, which is an improvement over the of 26% for the device with **DMAC-TRZ** (Error! Reference source not found.**7c**). The **CF_3Ph-DMAC-TRZ**, and **dPh-DMAC-TRZ** devices showed lower EQE_{max} of 18.5 and 21.6%, respectively, while the worst-performing device was the one with **CNPh-DMAC-TRZ**, with an EQE_{max} of 8.3%, which reflects the poor exciton harvesting ability of the emitter. These results are in good agreement with the photophysical properties of the six emitters. At 1000 cd m^{-2} the EQE of the six OLEDs was 20, 3.3, 12.8, 12.0, 21.5, and 22.1% for **DMAC-TRZ, CNPh-DMAC-TRZ**, **CF_3Ph-DMAC-TRZ**, **dPh-DMAC-TRZ**, **^{t}BuPh-DMAC-TRZ**, and **OMePh-DMAC-TRZ** respectively (Table **6**). This verifies that at higher current densities, the device roll-off is proportional to the triplet harvesting efficiency (k_{RISC}) of each individual emitter (**^{t}BuPh-DMAC-TRZ**, **OMePh-DMAC-TRZ** > **DMAC-TRZ** > **CF_3Ph-DMAC-TRZ**, **dPh-DMAC-TRZ** > **CNPh-DMAC-TRZ)**.

Table **2**. Performance metrics of the OLEDs.

Emitter	λ_{EL} / nm[a]	V_{on} / V	EQE_{max} / %	EQE_{1000} / %	CE_{max} / cd A^{-1}	PE_{max} / lm W^{-1}	L_{max} / cd m^{-2}	CIE (x, y)[a]	LT_{85} / h[a]
DMAC-TRZ	501	3.3	26	20	67	45.5	21,600	0.22; 0.48	1.1
CNPh-DMAC-TRZ	496	3.4	8.3	3.3	22.5	16	10,000	0.20; 0.39	0.9
CF_3Ph-DMAC-TRZ	498	3.3	18.5	12.8	54.6	40.8	13,200	0.22; 0.48	0.2
dPh-DMAC-TRZ	525	3.2	21.6	12.0	63	49.5	16,200	0.29; 0.55	1.9
^{t}BuPh-DMAC-TRZ	526	3.2	28	21.5	76.6	50.1	36,000	0.30; 0.56	0.6
OMePh-DMAC-TRZ	531	3.2	27.4	22.1	80.35	54.9	29,300	0.34; 0.57	0.3

[a] recorded at 10mA/cm^2, time necessary fort the emission intensity (I) to decrease to 85% of its initial value (I_0), I_0 is the luminance value taken at a current density of 10 mA/cm^2, which corresponds to 957, 2891, 2860, 4113, 5099, and 5743 cd m^{-2} for **CNPh-DMAC-TRZ**, **CF$_3$Ph-DMAC-TRZ**, **dPh-DMAC-TRZ**, **DMAC-TRZ**, **^{t}BuPh-DMAC-TRZ**, and **OMePh-DMAC-TRZ,** respectively.

Considering the variation of the EQE_{max} values across the OLEDs with the six emitters we have performed simulations of the light outcoupling factor as a function of TDM orientation (Figure **S43**). The light outcoupling efficiency was estimated to be 26, 22, 28, 24, 24 and 26%, for **CNPh-DMAC-TRZ**, **CF$_3$Ph-DMAC-TRZ**, **dPh-DMAC-TRZ**, **DMAC-TRZ, ^{t}BuPh-DMAC-TRZ**, and **OMePh-DMAC-TRZ**, respectively (Table **S8**). These results predict a small improvement of outcoupling efficiency in **CNPh-DMAC-TRZ**, **dPh-DMAC-TRZ**, and **OMePh-DMAC-TRZ** compared to **DMAC-TRZ**. However, despite their extended molecular length, the light outcoupling efficiencies of the devices with **CF$_3$Ph-DMAC-TRZ** and **^{t}BuPh-DMAC-TRZ** are, respectively, similar, or only slightly lower than the device with **DMAC-TRZ**. This makes the triplet harvesting efficiency of these emitters the main parameter that determines the EQE_{max} values of the devices. It is furthermore apparent from the light outcoupling simulations that the best devices with their measured EQEs in the range of 26-28% must basically have balanced carrier recombination as well as complete triplet harvesting.

Finally, the accelerated device lifetimes (at 10 mA cm^{-2} because of their different PL spectrum) were also assessed and the results shown in **Error! Reference source not found.**. Although the device lifetimes cannot be compared with industrial standards (or other highly optimised OLED studies), the lifetime trend is indicative. Most of the devices showed poorer lifetimes compared to the **DMAC-TRZ** OLEDs (**Error! Reference source not found.**), except the **dPh-DMAC-TRZ** devices with an almost double LT_{85} (1.1 h for **DMAC-TRZ** vs 1.9 h for **dPh-DMAC-TRZ**).The maximum luminance of each emitter is different at 10 mA cm^{-2}, which has an effect on the measured lifetime. To investigate the same luminance trend, we used lifetime extrapolation from the accelerated tests of DMAC-TRZ at different current densities (Figure **S45**). From this plot we can extract the estimated lifetime of DMAC-TRZ devices at different luminance, and the cross comparison with the other derivatives at the same luminance is shown in Table **S9**. The estimated lifetime of DMAC-TRZ is higher compared to all the other derivatives at the same luminance (but different current density) presumably because of its higher internal quantum efficiency and slightly different γ factor.

Conclusions

In this study we report five modified **DMAC-TRZ**[3] derivatives, **CNPh-DMAC-TRZ**, **CF_3Ph-DMAC-TRZ**, **dPh-DMAC-TRZ**, **^{t}BuPh-DMAC-TRZ**, and **OMePh-DMAC-TRZ**, bearing substituted acridine donors, to explore the impact of the substitution on their photophysical and orientation properties and the impact in the performance of the OLEDs. The emission was modulated from sky blue to green in 10 wt% doped films in mCBPCN as a function of the nature of the substituent. The trend in tuning the energy of the lowest singlet excited state did not match that tuning the energy of the lowest triplet excited state, as these states have contrasting charge-transfer and locally excited character, respectively. This behaviour results in a wide variation of the ΔE_{ST} across the five derivatives, and accordingly of k_{RISC} values (ranging from 10^3 to 10^6 s^{-1} for **CNPh-DMAC-TRZ** to **OMePh-DMAC-TRZ**, respectively), while the Φ_{PL} values are maintained around 70% in all compounds, except **CNPh-DMAC-TRZ** (34%) and **DMAC-TRZ** (87%). Angle-resolved PL measurements of the 10 wt% emitter in mCBPCN films revealed preferentially horizontally orientated TDMs for **CNPh-DMAC-TRZ**, **dPh-DMAC-TRZ**, and **OMe-DMAC-TRZ** compared to **DMAC-TRZ**; however, this is not the case for the **CF_3Ph-DMAC-TRZ** and **^{t}BuPh-DMAC-TRZ** films. This translates to a small improvement in the light outcoupling efficiency for the OLEDs with **CNPh-DMAC-TRZ**, **dPh-DMAC-TRZ**, and **OMe-DMAC-TRZ** (estimated from the light outcoupling simulations), compared to the device with **DMAC-TRZ**; however, this was not the case for the devices with **CF_3Ph-DMAC-TRZ** and **^{t}BuPh-DMAC-TRZ**.

Our study demonstrates that by decorating the donor with aryl groups in a D-A TADF emitter the probability of achieving a higher horizontal orientation of the TDM can be improved but is highly dependent on the nature of the attached aryl group. Nevertheless, the dominant effect on OLED efficiency results from triplet harvesting whereby **^{t}BuPh-DMAC-TRZ** and **OMe-DMAC-TRZ** have the fastest RISC rates and, consequently, show the highest EQE_{max} of ~28% and suppressed efficiency roll-off compared to the reference **DMAC-TRZ** OLEDs.

Acknowledgments

This project has received funding from the European Union's Horizon 2020 research and innovation programme under the Marie Skłodowska Curie grant agreement No 812872 (TADFlife). A.P.M. acknowledges the Engineering and Physical Sciences Research Council for funding through the grant EP/T02240X/1. E.Z.-C. acknowledges the Engineering and Physical Sciences Research Council for support through grants EP/P010482/1 and EP/W007517/1. W.B. acknowledges funding by Deutsche Forschungsgemeinschaft (DFG) under grant numbers 341263954 and 449697195.

Conflicts of interest

The authors declare no conflicts of interest.

Supporting Information

General methods; Experimental Section (^{1}H and ^{13}C NMR spectra, HRMS, EA and HPLC of all target compounds); supplementary computational data; supplementary photophysical data; supplementary OLED data; Outcoupling efficiency estimation; supplementary OLED lifetime data.

TOC

References

(1) Wong, M. Y.; Zysman-Colman, E. Purely Organic Thermally Activated Delayed Fluorescence Materials for Organic Light-Emitting Diodes. *Adv. Mater.* **2017**, *29*, 1605444. https://doi.org/10.1002/adma.201605444.

(2) Salehi, A.; Fu, X.; Shin, D. H.; So, F. Recent Advances in OLED Optical Design. *Adv. Funct. Mater.* **2019**, *29* (15), 1–21. https://doi.org/10.1002/adfm.201808803.

(3) Tsai, W. L.; Huang, M. H.; Lee, W. K.; Hsu, Y. J.; Pan, K. C.; Huang, Y. H.; Ting, H. C.; Sarma, M.; Ho, Y. Y.; Hu, H. C.; Chen, C. C.; Lee, M. T.; Wong, K. T.; Wu, C. C. A Versatile Thermally Activated Delayed Fluorescence Emitter for Both Highly Efficient Doped and Non-Doped Organic Light Emitting Devices. *Chem. Commun.* **2015**, *51* (71), 13662–13665. https://doi.org/10.1039/c5cc05022g.

(4) Naqvi, B. A.; Schmid, M.; Crovini, E.; Sahay, P.; Naujoks, T.; Rodella, F.; Zhang, Z.;

Strohriegl, P.; Bräse, S.; Zysman-Colman, E.; Brütting, W. What Controls the Orientation of TADF Emitters? *Front. Chem.* **2020**, *8*, 750. https://doi.org/10.3389/fchem.2020.00750.

(5) Stavrou, K.; Franca, L. G.; Monkman, A. P. Photophysics of TADF Guest-Host Systems: Introducing the Idea of Hosting Potential. *ACS Appl. Electron. Mater.* **2020**, *2* (9), 2868–2881. https://doi.org/10.1021/acsaelm.0c00514.

(6) Dhali, R.; Phan Huu, D. K. A.; Bertocchi, F.; Sissa, C.; Terenziani, F.; Painelli, A. Understanding TADF: A Joint Experimental and Theoretical Study of DMAC-TRZ. *Phys. Chem. Chem. Phys.* **2021**, *23* (1), 378–387. https://doi.org/10.1039/d0cp05982j.

(7) Wada, Y.; Kubo, S.; Kaji, H. Adamantyl Substitution Strategy for Realizing Solution-Processable Thermally Stable Deep-Blue Thermally Activated Delayed Fluorescence Materials. *Adv. Mater.* **2018**, *30* (8), 1705641. https://doi.org/10.1002/adma.201705641.

(8) Li, W.; Cai, X.; Li, B.; Gan, L.; He, Y.; Liu, K.; Chen, D.; Wu, Y. C.; Su, S. J. Adamantane-Substituted Acridine Donor for Blue Dual Fluorescence and Efficient Organic Light-Emitting Diodes. *Angew. Chemie - Int. Ed.* **2019**, *58* (2), 582–586. https://doi.org/10.1002/anie.201811703.

(9) Chen, W. C.; Lee, C. S.; Tong, Q. X. Blue-Emitting Organic Electrofluorescence Materials: Progress and Prospective. *J. Mater. Chem. C* **2015**, *3* (42), 10957–10963. https://doi.org/10.1039/c5tc02420j.

(10) Wada, Y.; Nakagawa, H.; Kaji, H. Acceleration of Reverse Intersystem Crossing Using Different Types of Charge Transfer States. *Chem. - An Asian J.* **2021**, *16* (9), 1073–1076. https://doi.org/10.1002/asia.202100091.

(11) Feng, Q.; Qian, Y.; Wang, H.; Hou, W.; Peng, X.; Xie, S.; Wang, S.; Xie, L. Donor Arylmethylation toward Horizontally Oriented TADF Emitters for Efficient Electroluminescence with 37% External Quantum Efficiency. *Adv. Opt. Mater.* **2022**, *10* (10), 1–9. https://doi.org/10.1002/adom.202102441.

(12) Tenopala-Carmona, F.; Lee, O. S.; Crovini, E.; Neferu, A. M.; Murawski, C.; Olivier, Y.; Zysman-Colman, E.; Gather, M. C. Identification of the Key Parameters for Horizontal Transition Dipole Orientation in Fluorescent and TADF Organic Light-Emitting Diodes. *Adv. Mater.* **2021**, *33* (2100677). https://doi.org/10.1002/adma.202100677.

(13) Liu, T.; Deng, C.; Duan, K.; Tsuboi, T.; Niu, S.; Wang, D.; Zhang, Q. Zero-Zero Energy-Dominated Degradation in Blue Organic Light-Emitting Diodes Employing Thermally Activated Delayed Fluorescence. *ACS Appl. Mater. Interfaces* **2022**, *14* (19), 22332–22340. https://doi.org/10.1021/acsami.2c02623.

(14) Adamo, C.; Barone, V. Toward Reliable Density Functional Methods without Adjustable Parameters: The PBE0 Model. *J. Chem. Phys.* **1999**, *110* (13), 6158–6170. https://doi.org/10.1063/1.478522.

(15) Dunning, T. H. Gaussian Basis Sets for Use in Correlated Molecular Calculations. I. The Atoms Boron through Neon and Hydrogen. *J. Chem. Phys.* **1989**, *90* (2), 1007–1023. https://doi.org/10.1063/1.456153.

(16) Furue, R.; Nishimoto, T.; Park, I. S.; Lee, J.; Yasuda, T. Aggregation-Induced Delayed Fluorescence Based on Donor/Acceptor-Tethered Janus Carborane Triads: Unique Photophysical Properties of Nondoped OLEDs. *Angew. Chemie - Int. Ed.* **2016**, *55* (25), 7171–7175. https://doi.org/10.1002/anie.201603232.

(17) Hsieh, Y. Y.; Sánchez, R. S.; Raffy, G.; Shyue, J. J.; Hirsch, L.; Del Guerzo, A.; Wong, K. T.; Bassani, D. M. Supramolecular Gating of TADF Process in Self-Assembled Nano-Spheres for High-Resolution OLED Applications. *Chem. Commun.* **2022**, *58* (8), 1163–1166. https://doi.org/10.1039/d1cc06120h.

(18) Zhang, Z.; Crovini, E.; dos Santos, P. L.; Naqvi, B. A.; Cordes, D. B.; Slawin, A. M. Z.; Sahay, P.; Brütting, W.; Samuel, I. D. W.; Bräse, S.; Zysman-Colman, E. Efficient Sky-Blue Organic Light-Emitting Diodes Using a Highly Horizontally Oriented Thermally Activated Delayed Fluorescence Emitter. *Adv. Opt. Mater.* **2020**. https://doi.org/10.1002/adom.202001354.

(19) Hundemer, F.; Crovini, E.; Wada, Y.; Kaji, H.; Bräse, S.; Zysman-Colman, E. Tris(Triazolo)Triazine-Based Emitters for Solution-Processed Blue Thermally Activated Delayed Fluorescence Organic Light-Emitting Diodes. *Mater. Adv.* **2020**, *1* (8), 2862–2871. https://doi.org/10.1039/d0ma00659a.

(20) Tsuchiya, Y.; Diesing, S.; Bencheikh, F.; Wada, Y.; dos Santos, P. L.; Kaji, H.; Zysman-Colman, E.; Samuel, I. D. W.; Adachi, C. Exact Solution of Kinetic Analysis for Thermally Activated Delayed Fluorescence Materials. *J. Phys. Chem. A* **2021**, *125* (36), 8074–8089. https://doi.org/10.1021/acs.jpca.1c04056.

(21) Mei, L.; Hu, J.; Cao, X.; Wang, F.; Zheng, C.; Tao, Y.; Zhang, X.; Huang, W. The Inductive-Effect of Electron Withdrawing Trifluoromethyl for Thermally Activated Delayed Fluorescence: Tunable Emission from Tetra- to Penta-Carbazole in Solution Processed Blue OLEDs. *Chem. Commun.* **2015**, *51* (65), 13024–13027. https://doi.org/10.1039/c5cc04126k.

(22) Yang, J.; Fang, M.; Li, Z. Organic Luminescent Materials: The Concentration on Aggregates from Aggregation-Induced Emission. *Aggregate* **2020**, *1* (1), 6–18. https://doi.org/10.1002/agt2.2.

(23) Bardi, B.; Giavazzi, D.; Ferrari, E.; Iagatti, A.; Di Donato, M.; Phan Huu, D. K. A.; Di Maiolo, F.; Sissa, C.; Masino, M.; Lapini, A.; Painelli, A. Solid State Solvation: A Fresh View. *Mater. Horizons* **2023**, *10* (10), 4172–4182. https://doi.org/10.1039/d3mh00988b.

(24) Dianming Sun, Eimantas Duda, Xiaochun Fan, Rishabh Saxena, Ming Zhang, Sergey Bagnich, Xiaohong Zhang, Anna Köhler, and E. Z.-C. Thermally Activated Delayed Fluorescent Dendrimers That Underpin High-Efficiency Host-Free Solution-Processed Organic Light-Emitting Diodes. *Adv. Mater.* **2022**, *34*, 2110344. https://doi.org/10.1002/adma.202110344.

(25) Chatterjee, T.; Wong, K. T. Perspective on Host Materials for Thermally Activated Delayed Fluorescence Organic Light Emitting Diodes. *Adv. Opt. Mater.* **2019**, *7* (1), 1–34. https://doi.org/10.1002/adom.201800565.

(26) Stavrou, K.; Franca, L. G.; Böhmer, T.; Duben, L. M.; Marian, C. M.; Monkman, A. P. Unexpected Quasi-Axial Conformer in Thermally Activated Delayed Fluorescence DMAC-TRZ, Pushing Green OLEDs to Blue. *Adv. Funct. Mater.* **2023**, *33* (25). https://doi.org/10.1002/adfm.202300910.

(27) Dias, F. B.; Penfold, T. J.; Monkman, A. P. Photophysics of Thermally Activated Delayed Fluorescence Molecules. *Methods Appl. Fluoresc.* **2017**, *5* (1), 012001. https://doi.org/10.1088/2050-6120/aa537e.